Electrochimica Acta 100 (2013) 78–84

Contents lists available at SciVerse ScienceDirect

Electrochimica Acta

journal homepage: www.elsevier.com/locate/electacta

Mass-transfer studies in an electrochemical reactor with a small interelectrode gap

A.N. Colli[a], R. Toelzer[b], M.E.H. Bergmann[b], J.M. Bisang[a,*]

[a] Universidad Nacional del Litoral, Santiago del Estero 2829, S3000AOM Santa Fe, Argentina
[b] Anhalt University, Bernburger Str. 55, D-06366 Köthen (Anhalt), Germany

ARTICLE INFO

Article history:
Received 26 December 2012
Received in revised form 15 March 2013
Accepted 21 March 2013
Available online 1 April 2013

Keywords:
Drinking water disinfection
Flow reactors
Mass-transfer coefficient
Parallel-plate electrodes
Turbulence promoter

ABSTRACT

This paper reports the distribution of the local mass-transfer coefficient along the electrode length for an electrochemical reactor with parallel-plate electrodes and narrow interelectrode gaps of 1 and 2.2 mm, using the reduction of ferricyanide as a test reaction. The studies were performed at different flow rates, Reynolds numbers ranging from 370 to 3700, with the empty reactor and also the interelectrode gap was filled with two types of expanded plastics and a woven plastic mesh as turbulence promoters. The effect of both the interelectrode gap and the partial placing of the turbulence promoter along the electrode length on the mass-transfer behaviour was also analyzed. In all cases the pressure drop across the reactor was measured. A more uniform distribution of the local mass-transfer coefficient, ±15% related to its mean value, and an important increase of the mean mass-transfer coefficient, enhancement factor ranging from 2 to 8, were observed, depending on the type of turbulence promoter, the volumetric flow rate, and the interelectrode gap.

1. Introduction

Electrochemical reactors with parallel-plate electrodes are the most common cell arrangement used in the industrial practice either in monopolar or bipolar connection. In the design of these devices three aspects are of capital importance: (i) to obtain high mean values of the mass-transfer coefficient, (ii) to achieve a uniform local mass-transfer coefficient along the electrode length and (iii) to minimize the entrance and exit effects, which requires to paid special attention to the design of the inlet and outlet of the electrolyte to the reactor. In order to address the above issues, flow obstacles are placed in the interelectrode gap to promote turbulence [1], becoming the turbulence promoter an essential part in the design of the electrochemical reactor. Thus, Cœuret and Storck [2] summarized mass-transfer correlations for different turbulence promoters. Related to electrochemical reactors with parallel-plate electrodes, Storck et al. [3,4] studied the mass-transfer and pressure drop performance of cylindrical promoters placed in the middle of a channel, 10 mm thick, or against the electrode surface and plastic meshes positioned close to the electrodes. They obtained the local mass-transfer coefficient distribution using an arrangement of microelectrodes. Mass-transfer studies have also been informed for a commercial filter-press reactor with an interelectrode gap of 9 mm, the ElectroSyncell® cell [5]; where a specially designed plastic grid with triangular threads attached to the electrodes, SU-grid, and cylindrical rods placed perpendicularly to the direction flow in the middle of the flow channel were examined as turbulence promoters. It was reported that this grid is a very efficient one, increasing the mass-transfer coefficient from 3 to 6 times, depending on the flow rate. The study of the mass-transfer characteristics of various mesh spacers for electrodialysis demonstrated that more effective promoters can be developed by adjusting mesh sizes [6]. The effect of expanded metals coated with a nonconducting paint, as turbulence promoting structures, on the mass-transfer in a thin channel was performed with interelectrode gaps ranging from 0.7 to 2 mm [7]. Mass-transfer enhancement factors ranging from 1.05 to 2.20 were reported using eight different turbulence promoters in a divided electrochemical reactor [8] whose catholite chamber, 20 mm thick, was completely filled with the promoter. Studies performed with a DEM electrochemical cell [9] concluded that the use of a turbulence promoter increases the mass-transfer rates by 50–100% and becomes more uniform its distribution over the electrode surface Likewise, the study of the effect of a variety of wall obstructions on local mass-transfer in a parallel plate electrochemical flow cell of 10 mm interelectrode space [10] concluded that the mass-transfer rate depends on the type and size of the obstruction and its position in the channel flow. The turbulence promoting action of plastic meshes, 5.5 mm thick, and a stack of fine plastic nets with the same thickness on the mass-transfer behaviour in the so-called FM01-LC reactor was reported by Brown et al. [11,12] and its effect on the global mass-transfer coefficient using the first turbulence promoter at high mean fluid

* Corresponding author. Tel.: +54 342 4571164; fax: +54 342 4571164.
E-mail address: jbisang@fiq.unl.edu.ar (J.M. Bisang).

0013-4686/$ – see front matter © 2013 Elsevier Ltd. All rights reserved.
http://dx.doi.org/10.1016/j.electacta.2013.03.134

velocity by Griffiths et al. [13]. The influence of parameters such as shape, orientation and dimensions of mesh-type spacers on the mass-transfer behaviour focussed to membrane separation processes was also analyzed [14,15]. The modification of the velocity field by putting some obstacles of different shapes and sizes in the flow path of the electrolyser was also numerically simulated [16].

Likewise, the interelectrode gap must be small to diminish the ohmic drop in the solution phase, which becomes more important for the processing of low conductivity electrolytes as in the reactors for organic electrosynthesis, electrodialysis and for drinking water disinfection. This last method has recently received significant attention in the literature [17]. It represents a convenient and highly efficient way to produce germ-free water by using an electric current passed through the water under treatment by means of suitable electrodes, without the external addition of chemical compounds [18,19].

Some of the above works recognized the efficiency of the expanded structures to increase the mean mass-transfer coefficient. Thus, the main aim of the present paper is to give further experimental results about the effect of turbulence promoters on the local and mean mass-transfer coefficients focusing the attention in parallel plate electrochemical reactors with a narrow interelectrode gap, typical of the devices used in electrochemical water disinfection.

2. Experimental

All experiments were performed in an electrochemical reactor with parallel plate electrodes, as shown in Fig. 1. The reactor was made of acrylic material with both electrodes of nickel, 100 mm wide and 250 mm long, arranged in a filter press configuration. This reactor has the same aspect ratio as that of our previous work [19]. The anode, a sheet of 1 mm thick, was electrically fed along its two lateral sides by means of copper current feeders, which were connected to the dc power supply at both ends to ensure isopotentiality of the metal phase. The cathode was made of 25 nickel segments, 100 mm wide, 9.5 mm long and 1 mm thick, which were insulated from one another by an epoxy resin of about 0.5 mm thick. The surface of the working electrode was polished to a bright mirror finish with slurry of 0.3 μm alumina powder and it was washed with distilled water. Calibrated resistors, 0.026 Ω resistance, were inserted between the backside of each segment and the cathodic current feeder, which was electrically connected at both ends. By measuring the ohmic drop in the resistors, it was possible to determine the axial current distribution and to calculate the local mass-transfer coefficient. The effect of the calibrated resistors on the current distribution can be neglected due to the small value of their ohmic drop, approximately 10 mV, in comparison with the other terms of the voltage balance in the reactor. Likewise, the variation of the local mass-transfer along the electrode width can be disregarded due to the small ratio between the interelectrode gap and the electrode width [20]. The data acquisition was performed using a computer controlled, home made analogue multiplexer. The experiments were carried out potentiostatically at potentials ranging from −0.1 V to −0.4 V to verify that a limiting current was achieved. The cathodic potential was controlled against a saturated calomel electrode connected to a Haber–Luggin capillary positioned in the middle region of the cathode. However, the cathodic potential was also measured near the reactor entrance and at the reactor exit in order to insure that all the segments in the cathode were under limiting current conditions. These ports were also used in additional experiments to measure the pressure drop across the reactor with a manometer. The lower and upper parts of the reactor present chambers, of triangular cross-sectional area, with perpendicular nozzles for the inlet and outlet of the

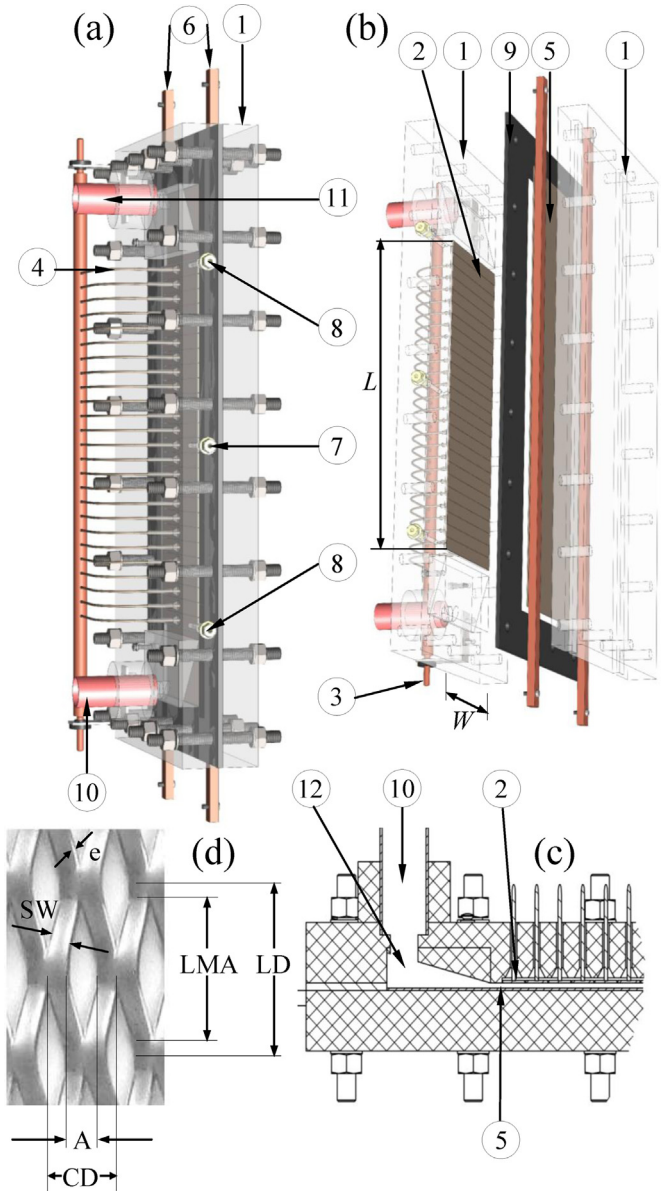

Fig. 1. (a) Schematic representation of the parallel plate electrochemical reactor. (b) Exploded view of the reactor. (c) Cross-section showing the electrolyte inlet chamber in the reactor. (d) View of the expanded plastic mesh with the characteristic parameters according to Table 1. 1, plates; 2, segmented electrodes; 3, current feeder to the working electrode; 4, calibrated resistors; 5, counterelectrode; 6, electrical connection to the counterelectrode; 7, Luggin capillary for potential control; 8, Luggin capillaries for potential measurements and ports for pressure drop measurement; 9, gasket; 10, electrolyte inlet; 11, electrolyte outlet; 12, electrolyte inlet chamber.

electrolyte, which is represented in the exploded view of Fig. 1(c). The counterelectrode in the inlet and outlet chambers was coated with a silicone-based resin in order to make it non-conductive. Two interelectrode gaps were used, 1.0 and 2.2 mm, which were fixed by the thickness of the gasket. The same reactor was used in our previous paper [21], where it was possible to predict the mass-transfer behaviour without turbulence promoters under laminar flow conditions using theoretical velocity profiles. It was concluded that the flow distributors are properly designed and the mass-transfer measurements are scarcely influenced by the entrance and exit effects. Two types of turbulence promoters were used: expanded plastic meshes (EPM), and a woven plastic mesh (WPM). The geometrical characteristics, measured in the laboratory and defined in Fig. 1 (d), are summarized in Table 1. The expanded

Table 1
Geometrical parameters of the turbulence promoters.

Characteristic parameters of the expanded plastic mesh (EPM)	EPM1	EPM2
Long diagonal, LD/mm	21	16.2
Short diagonal, CD/mm	5.5	11.5
Long mesh aperture, LMA/mm	12.5	11.0
Short mesh aperture, *A*/mm	3	9.5
Thickness, *e*/mm	1.2	0.5
Apparent thickness, (1 sheet)/mm	2.4	1.2
Strand width, SW/mm	1.8	1.0
Specific surface area, A_s/m	1015	571
Porosity, ε	0.67	0.85

Characteristic parameters of woven plastic mesh (WPM)	
Thread, diameter/mm	0.4
Mesh, size/mm	1.29 × 1.55
Specific surface area, A_s/m	2240
Porosity, ε	0.72

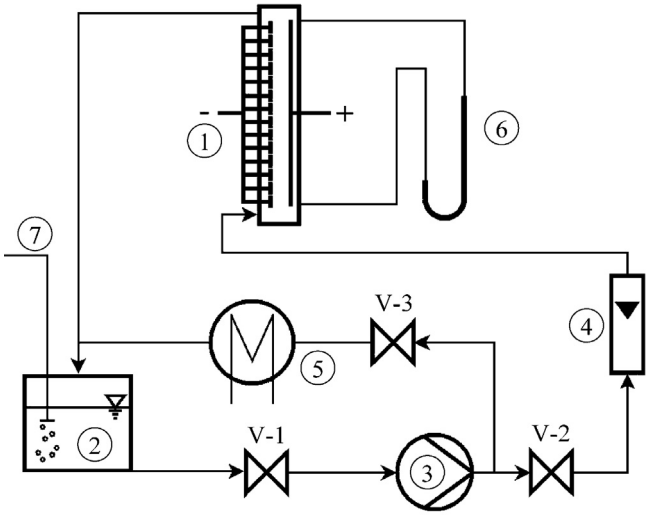

Fig. 2. Scheme of the electrolyte circulation system. 1, electrochemical reactor; 2, reservoir; 3, pump; 4, flowmeter; 5, thermostat; 6, manometer; 7, inlet of nitrogen; V-1, V-2, V-3, valves.

plastic meshes were placed in the interelectrode gap with the long diagonal in the direction of the electrolyte flow. Likewise, experiments were also performed with segments of turbulence promoter positioned at different places along the electrode length.

The reactor was made part of a flow circuit system, sketched in Fig. 2, consisting of a pump, a flowmeter, a reservoir and connections to maintain the temperature at the preset value, 30 °C. Experiments were carried out with upwards and downwards flow of the electrolyte. The test reaction was the electrochemical reduction of ferricyanide from freshly prepared solutions with $[K_3Fe(CN)_6] \cong 0.1\ mol\ dm^{-3}$, $[K_4Fe(CN)_6] \cong 0.1\ mol\ dm^{-3}$, in $0.5\ mol\ dm^{-3}$ of NaOH as supporting electrolyte, while the reverse reaction occurred at the anode. Table 2 summarizes the composition and physicochemical properties of the electrolyte. Samples of

Table 2
Properties of the electrolyte.

Composition	$[K_3Fe(CN)_6] = 0.1$ M $[K_4Fe(CN)_6] = 0.1$ M [NaOH] = 0.5 M
Kinematic viscosity, $\nu/m^2\ s^{-1}$	8.80×10^{-7}
Diffusion coefficient, $D/m^2\ s^{-1}$	7.50×10^{-10}
Sc	1173

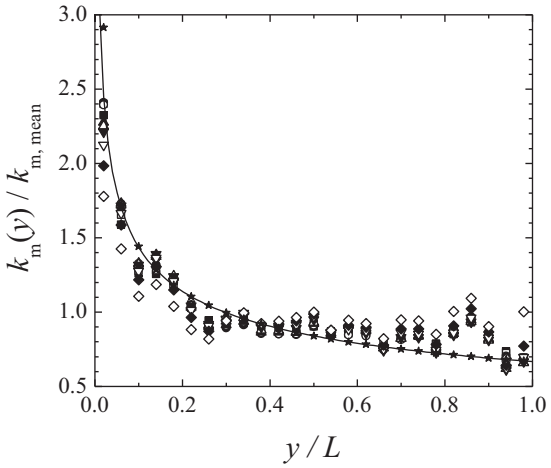

Fig. 3. Ratio between the local mass-transfer coefficient to the mean value as a function of the axial position for the empty reactor at different volumetric flow rates. (■) $1.67 \times 10^{-5}\ m^3\ s^{-1}$. (□) $3.33 \times 10^{-5}\ m^3\ s^{-1}$. (●) $5 \times 10^{-5}\ m^3\ s^{-1}$. (○) $6.67 \times 10^{-5}\ m^3\ s^{-1}$. (▲) $8.33 \times 10^{-5}\ m^3\ s^{-1}$. (△) $1.0 \times 10^{-4}\ m^3\ s^{-1}$. (▼) $1.17 \times 10^{-4}\ m^3\ s^{-1}$. (▽) $1.33 \times 10^{-4}\ m^3\ s^{-1}$. (♦) $1.5 \times 10^{-4}\ m^3\ s^{-1}$. (◊) $1.67 \times 10^{-4}\ m^3\ s^{-1}$. Reynolds number based on hydraulic diameter ranging from 371 to 3713. Full line: theoretical behaviour for a parallel plate electrochemical reactor with infinitely wide electrodes and fully developed laminar flow, Eq. (2). (⋆) Dimensionless mean mass-transfer coefficient at each segment according to Eq. (2). Upwards flow. Interelectrode gap: 2.2 mm.

the solution were taken from the reactor after each experiment and the ferricyanide concentration was spectrophotometrically determined using a Perkin-Elmer model Lambda 20 double-beam UV–Vis spectrophotometer with 10 mm glass absorption cells and the supporting electrolyte was used as blank. The measurements were performed at a wavelength of 420 nm, where it is possible to determine the ferricyanide concentration without any interference of ferrocyanide. Nitrogen was bubbled in the reservoir for 1 h prior to the experiment in order to remove the dissolved oxygen.

The mass-transfer coefficient was calculated from the limiting current and the reactant concentration using the following equation [22]:

$$k_m = \frac{I_{lim}}{\nu_e F W l c} \tag{1}$$

where I_{lim} is the limiting current at each segment, *l* is the segment length, *W* is the electrode width, *c* is the bulk concentration of the electroactive species, ν_e is the number of electrons interchanged and *F* is the Faraday constant.

3. Results and discussion

Fig. 3 shows, for the empty reactor, the ratio between the local mass-transfer coefficient, k_m, and the mean value for the total electrode, $k_{m,\ mean}$, as a function of the axial position, *y*, at different volumetric flow rates, *Q*. Empty reactor denotes the equipment without turbulence promoters in the interelectrode gap. The full line represents the theoretical behaviour for a parallel plate electrochemical reactor with infinitely wide electrodes and fully developed laminar flow, according to the following equation [20]:

$$\frac{k_m(y)}{k_{m,mean}} = \frac{2}{3}\left(\frac{1}{y/L}\right)^{1/3} \tag{2}$$

being *L* the electrode length. The use of a segmented electrode allows to calculate the mean mass-transfer coefficient at each segment, which approaches the local value when smaller is the size of the segment. The dimensionless mean values at each segment, calculated with Eq. (2), are reported as full stars in Fig. 3, where

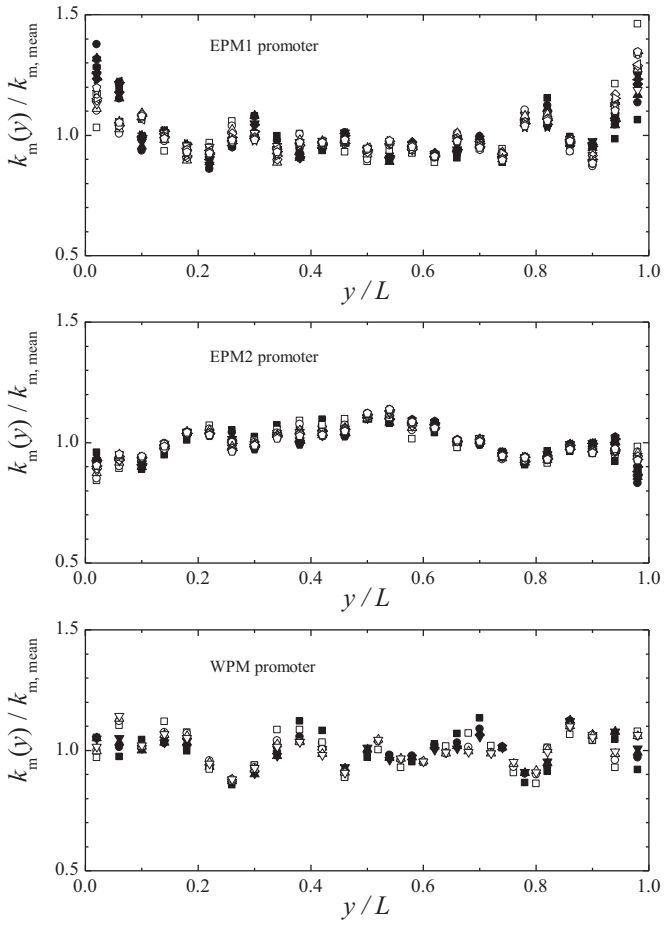

Fig. 4. Ratio between the local mass-transfer coefficient to the mean value as a function of the axial position in the reactor for different turbulence promoters. The symbols at each figure correspond to different volumetric flow rates according to: (■) and (□) 1.67×10^{-5} m^3 s^{-1}. (●) and (○) 3.33×10^{-5} m^3 s^{-1}. (▲) and (△) 5×10^{-5} m^3 s^{-1}. (▼) and (▽) 6.67×10^{-5} m^3 s^{-1}. (♦) and (◊) 8.33×10^{-5} m^3 s^{-1}. (◄) and (◁) 1.0×10^{-4} m^3 s^{-1}. (►) and (▷) 1.17×10^{-4} m^3 s^{-1}. (⬢) and (○) 1.33×10^{-4} m^3 s^{-1}. (★) and (☆) 1.5×10^{-4} m^3 s^{-1}. (⬟) and (○) 1.67×10^{-4} m^3 s^{-1}. Full symbols: upwards flow. Open symbols: downwards flow. Interelectrode gap: 2.2 mm.

no important difference between mean and local theoretical data can be observed. Then, it is concluded that the size of the segments is appropriate to determine local mass-transfer coefficients. The experimental results approach the theoretical model, which demonstrates that the special design of the chambers for the inlet and outlet of the electrolyte produces an efficient distribution of the electrolyte flow. Small deviations between experimental and theoretical data in the reactor entrance at low flow rates can be expected because of the developing flow conditions in this region [21] and at volumetric flow rates higher than 8.33×10^{-5} m^3 s^{-1} the discrepancy increases due to that the flow becomes turbulent. Likewise, a small peak, characteristic of an edge effect, is observed near the reactor exit caused by the change of flow area. It can be detected a pronounced variation of the local mass-transfer coefficient with the axial position. Thus, the mass-transfer coefficient at the reactor inlet is two and a half times its mean value.

Fig. 4 shows the ratio between the local mass-transfer coefficient and its mean value as a function of the axial position in the reactor for different turbulence promoters. For the EPM turbulence promoters the volumetric flow rate ranges from 1.67×10^{-5} m^3 s^{-1} to 1.67×10^{-4} m^3 s^{-1} and for the WPM one from 1.67×10^{-5} m^3 s^{-1} to 6.67×10^{-5} m^3 s^{-1}, because of the higher pressure drop of this structure. The comparison with the experimental results for the

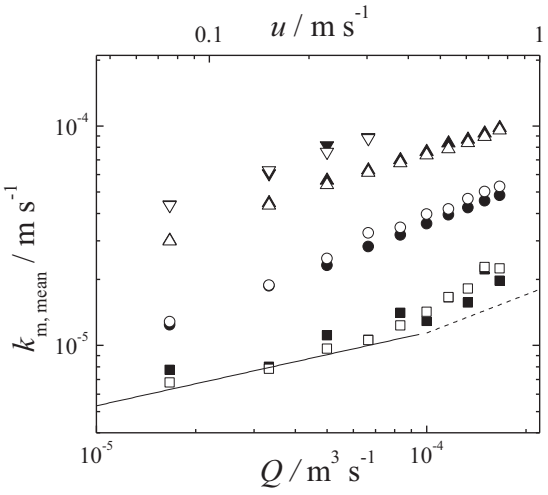

Fig. 5. Mean value of the mass-transfer coefficient as a function of the volumetric flow rate for different turbulence promoters. Full symbols: upwards flow. Open symbols: downwards flow. (■) and (□) empty reactor. (●) and (○) EPM1 turbulence promoter. (▲) and (△) EPM2 turbulence promoter. (▼) and (▽) WPM turbulence promoter. Full line: theoretical behaviour under laminar flow, Eq. (3). Dashed line: turbulent flow according to Eq. (4). Interelectrode gap: 2.2 mm.

empty reactor, Fig. 3, shows that the turbulence promoters become more uniform the mass-transfer coefficient along the reactor length. The standard deviations were 0.09989, 0.06123 and 0.06519 for the EPM1, EPM2 and WPM turbulence promoters, respectively. A scattering of ±15% related to its mean value is observed for the last two turbulence promoters and the EPM1 promoter presents a higher deviation but only at the entrance and exit regions of the reactor. Fig. 5 shows the mean mass-transfer coefficient as a function of the volumetric flow rate for the empty reactor and with the three turbulence promoters. The superficial liquid flow velocity, u, is also given, defined as the quotient between the volumetric flow rate and the cross-sectional area for the electrolyte flow in the empty reactor. The full line represents the behaviour for an empty reactor with infinitely wide electrodes and fully developed laminar flow, according to the following equation [20]:

$$k_{m,mean} = 1.85 \frac{D}{d_h} \left(\frac{d_h^2 Q}{\nu SWL} Sc \right)^{1/3} \quad (3)$$

and the dashed line under turbulent flow in accordance with [23]:

$$k_{m,mean} = 0.275 \frac{D}{d_h} \left(\frac{d_h Q}{\nu SW} \right)^{0.58} \left(\frac{d_h}{L} Sc \right)^{1/3} \quad (4)$$

here D is the diffusion coefficient of ferricyanide ions in the solution, ν is the kinematic viscosity, and S is the interelectrode gap. The hydraulic diameter, d_h, and Schmidt number, Sc, are defined by

$$d_h = \frac{2SW}{S+W} \quad (5)$$

$$Sc = \frac{\nu}{D} \quad (6)$$

A satisfactory agreement between experimental and theoretical results is observed for the empty reactor and in all cases no important difference is detected with the change of the electrolyte flow direction. The mass-transfer results for the turbulence promoters are summarized in Table 3 as dimensionless correlations. The WPM turbulence promoter exhibits the highest values in the mean mass-transfer coefficient. However, it has been tested only in laminar flow due to the volumetric flow rate is limited by the high pressure drop across the reactor, which represents a drawback

Table 3
Summary of correlation parameters.

	$Sh = Constant\ Re^a Sc^{1/3}$	
	Constant	a
EPM1	0.17	0.61
EPM2	0.80	0.50
WPM	1.01	0.52

$Sh = k_m\, d_h/D$ and $Re = u\, d_h/\nu$.

for this turbulence promoter. Moreover, the study of the residence time distribution in an electrochemical reactor filled with woven plastic meshes showed an inappropriate hydrodynamic behaviour characterized by the formation of by-pass channels [24]. Thus, from Figs. 4 and 5, the EPM2 turbulence promoter can be identified as the best choice, because it offers as advantages a higher value of the mean mass-transfer coefficient under laminar and turbulent flow conditions and also the more uniform local mass-transfer coefficient, corroborated by the lowest standard deviation.

Fig. 6 reports the variation of the ratio between the local mass-transfer coefficient and its mean value for two interelectrode gaps using the EPM2 turbulence promoter. The points represent the mean value measured at different volumetric flow rates, $1.67 \times 10^{-5} - 1.67 \times 10^{-4}\ m^3\ s^{-1}$ for 2.2 mm interelectrode gap and 1.67×10^{-5} to $1.17 \times 10^{-4}\ m^3\ s^{-1}$ for 1 mm, and the segments correspond to its standard deviation. Likewise, for 2.2 mm interelectrode gap the standard deviation of the mean values is 0.05973 and 0.09213 for the small one, demonstrating that a more uniform mass-transfer distribution is achieved at the largest interlectrode gap. Fig. 7 reports, for the EPM2 turbulence promoter, the mean mass-transfer coefficient as a function of the superficial liquid flow velocity where no effect of the interelectrode gap is observed. From Figs. 6 and 7 it can be concluded that the use of a large interelectrode gap presents as beneficial aspects a smaller variation of the local mass-transfer coefficient along the reactor length, similar values of the mean mass-transfer coefficients and it is also expected lower pressure drops. However, a large interelectrode gap shows as drawback high ohmic drop in the solution phase increasing the cell voltage, which is detrimental for the specific energy consumption of the reactor. Therefore, the adoption of the interelectrode gap must be an economic compromise between these opposite effects depending on each particular case.

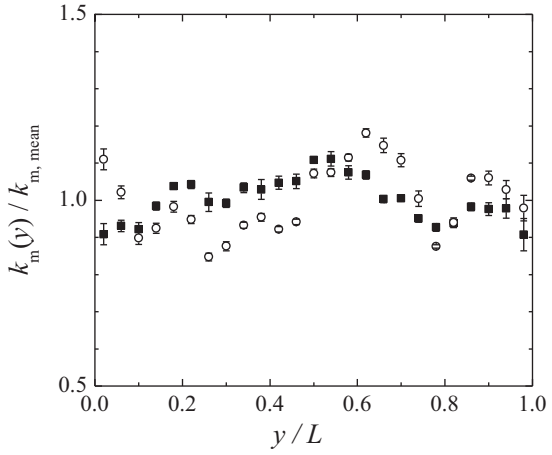

Fig. 6. Ratio between the local mass-transfer coefficient to the mean value as a function of the axial position in the reactor for different interelectrode gaps. Experimental points: mean value at different volumetric flow rates. (○) 1 mm interelectrode gap. (■) 2.2 mm interelectrode gap. Segments: standard deviation. Type of turbulent promoter: EPM2.

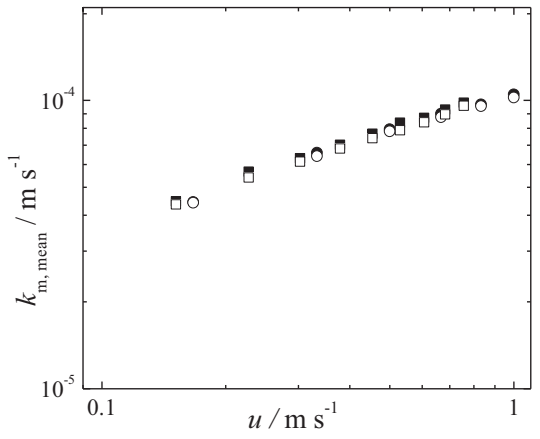

Fig. 7. Mean value of the mass-transfer coefficient as a function of the superficial liquid flow velocity for two interelectrode gaps. (●) and (○) 1 mm interelectrode gap. (■) and (□) 2.2 mm interelectrode gap. Full symbols: upwards flow. Open symbols: downwards flow. Type of turbulent promoter: EPM2.

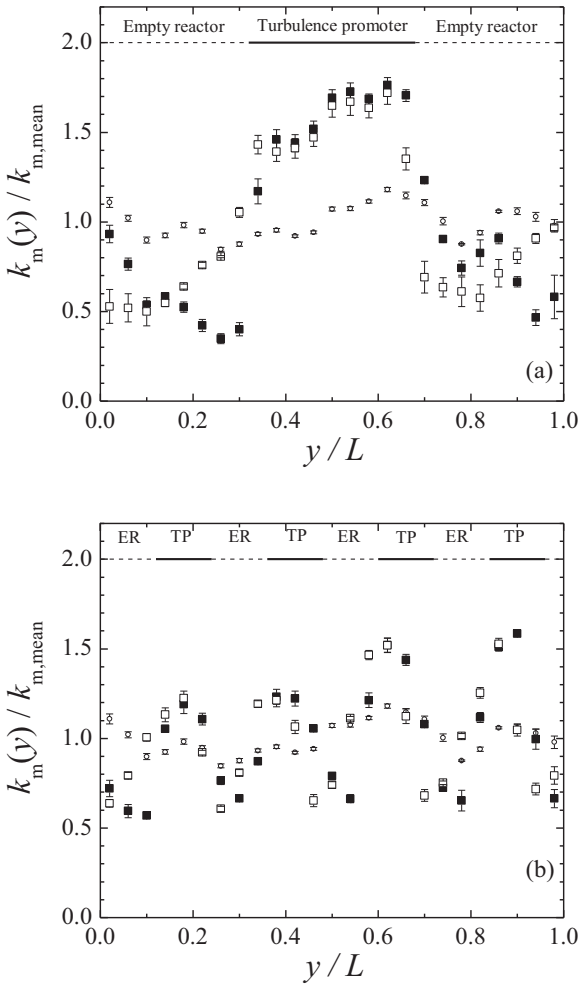

Fig. 8. Effect of the length of the turbulence promoter on the ratio between the local mass-transfer coefficient to the mean value as a function of the axial position in the reactor. Part (a): the turbulence promoter is set on the middle part of the electrode. Part (b): four pieces of turbulence promoter placed on the electrode surface. The position of the turbulence promoter is shown in the upper part at each figure. ER: empty reactor. TP: turbulence promoter. (○) Turbulence promoter is set on the entire electrode surface. (■) Upwards flow. (□) Downwards flow. Segments: standard deviation. Type of turbulence promoter: EPM2. Interelectrode gap: 1 mm. Volumetric flow rate range: 1.67×10^{-5}–$1.17 \times 10^{-4}\ m^3\ s^{-1}$.

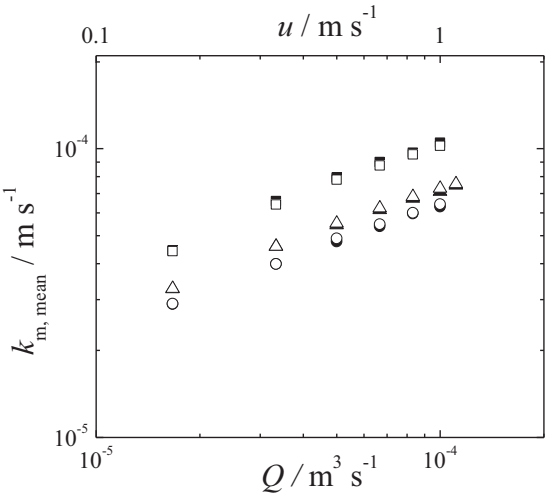

Fig. 9. Mean value of the mass-transfer coefficient as a function of the volumetric flow rate for the EPM2 turbulence promoter with a partial placing at the electrode surface in different forms. Full symbols: upwards flow. Open symbols: downwards flow. (■) and (□) Turbulence promoter is set on the entire electrode surface. (●) and (○) The turbulence promoter is set on the middle part of the electrode, Fig. 8(a). (▲) and (△) Four pieces of turbulence promoter placed on the electrode surface, Fig. 8(b). Interelectrode gap: 1 mm.

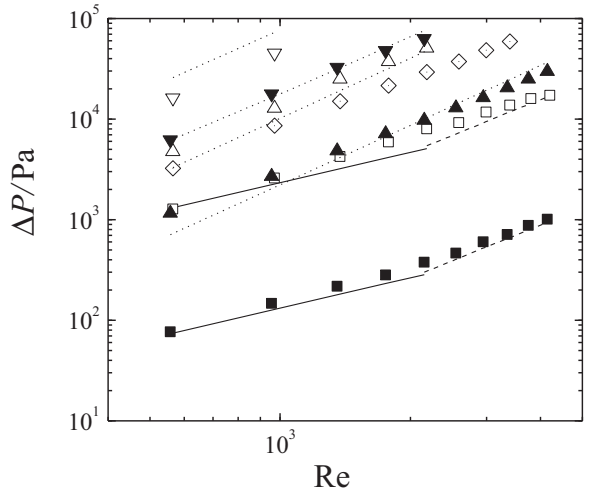

Fig. 10. Pressure drop across the reactor as a function of the Reynolds number for two interelectrode gaps. Full symbols: 2.2 mm interelectrode gap. Open symbols: 1 mm interelectrode gap. (■) and (□) Empty reactor. (▲) and (△) EPM2 turbulence promoter. (◈): EPM2 turbulence promoter according to Fig. 8. (▼) and (▽): WPM turbulence promoter. Full lines: theoretical behaviour under laminar flow, Eq. (7). Dashed lines: turbulent flow according to Eq. (8). Dotted lines: according to Eq. (9) for the interelectrode gap completely filled with the turbulence promoter.

Fig. 8 shows the influence of the length of the EPM2 turbulence promoter on the ratio between the local mass-transfer coefficient to its mean value. The volumetric flow range was between 1.67×10^{-5} and $1.17 \times 10^{-4}\ m^3\ s^{-1}$. The symbol (◯) corresponds to the case reported in Fig. 6 for 1 mm interelectrode gap, which is included as a baseline for performance comparison. Fig. 9 reports the mean value of the mass-transfer coefficient for the cases informed in Fig. 8. The dependence with the electrolyte flow direction shown in Fig. 8(b), can be attributed to that the turbulence promoter is not symmetrically placed in relation to the top and bottom of the reactor. Likewise, the mass-transfer distribution becomes more non-uniform when the turbulence promoter is partially placed on the electrode surface and the maximum values of the local mass-transfer coefficient are observed in the electrode regions with the turbulence promoter. However according to Fig. 9, the mean mass-transfer coefficient is not affected by the flow direction and the higher values are detected when the turbulence promoter is put on the total electrode surface.

The pressure drop across the reactor for the different arrangements is given in Fig. 10 as a function of the Reynolds number, $Re = u\, d_h/\nu$. The full lines represent the theoretical behaviour for a parallel plate reactor with infinitely wide electrodes and fully developed laminar flow according to [25]:

$$\Delta P = 4\frac{24}{Re}\frac{L}{d_h}\frac{\rho u^2}{2} \tag{7}$$

being ρ the density. For smooth parallel plate electrodes under developed turbulent flow the pressure drop is given by [26]:

$$\Delta P = 4\frac{0.08}{Re^{1/4}}\frac{L}{d_h}\frac{\rho u^2}{2} \tag{8}$$

The pressure drop for the reactor filled with turbulence promoters was calculated with the Ergun equation [26]:

$$\Delta P = \frac{A_s L}{3\varepsilon^3}\left(1.75 + \frac{25 A_s d_h}{Re}\right)\frac{\rho u^2}{2} \tag{9}$$

here A_s is the specific surface area of the promoter and ε is the porosity.

A close agreement is observed between Eqs. (7)–(9) with the experimental pressure drops at both interelectrode gaps. Likewise, as expected the pressure drop across the reactor increases when the interelectrode gap decreases and it is also observed a strong dependence on the geometry of the turbulence promoter. However, no influence on the pressure drop was detected for the different arrangements of the turbulence promoter, Fig. 8, partially placed on the electrode surface.

The mass-transfer enhancement factor, which relates the mean mass-transfer coefficient in the presence of a turbulence promoter to the value for the empty reactor, is reported in Fig. 11 in terms

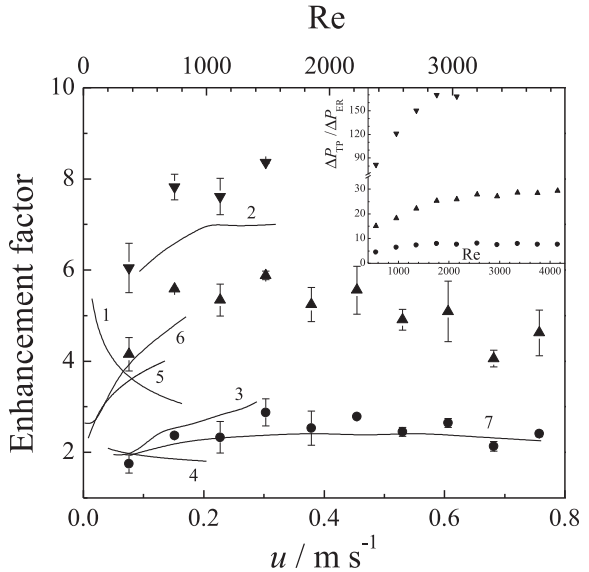

Fig. 11. Enhancement factor as a function of the superficial liquid flow velocity and Reynolds number. (●) EPM1 turbulence promoter. (▲) EPM2 turbulence promoter. (▼) WPM turbulence promoter. Segments: standard deviation. Inset: ratio between the pressure drop across the reactor with turbulence promoter and the value for the empty reactor as a function of the Reynolds number. Interelectrode gap: 2.2 mm. Full lines show the enhancement factors from previous studies for typical turbulence promoters. (1): SU-grid from [5]. (2): SU-grid from [7]. (3): expanded metal coated with a nonconducting paint from [7]. (4): six kinds of plastic meshes from [12]. (5): diamond-shape plastic meshes from [6]. (6): diamond-shape plastic meshes from [15]. (7): reticulated vitreous carbon electrode from [27].

of the superficial liquid flow velocity and Reynolds number for the examined cases with 2.2 mm interelectrode gap. The enhancement factor from previous studies, related to the corresponding empty reactor, for typical turbulence promoters and also for a three dimensional electrode of reticulated vitreous carbon [27] is included for comparison as full lines in the range of tested Reynolds numbers, where a high scattering of the data can be observed. Comparing the results for the SU-grid according to [5] and [7] a different behaviour is observed. The same conclusion can be achieved analyzing the data from [6,12,15], where similar turbulence promoters were investigated. Thus, the same turbulence promoter tested in different reactors shows a different behaviour, which can be attributed to the hydrodynamic conditions inside each equipment because of their different geometric configurations. Taking into account the small aspect ratios, interelectrode gap/electrode width, and the similar values of the reactor lengths, the flow distributors for the inlet and outlet of the solution can be considered as the predominant geometric parameter, which produces entrance and exit effects that modify the hydrodynamics of the empty reactor and also disturb the mass-transfer performance of the turbulence promoter. Then, for the mass-transfer characterization of turbulence promoters it is necessary to use reactors with well designed flow distributors to avoid distortion of the results by the edge effects, which are more significant for the small equipments used in laboratory measurements [28]. The inset in Fig. 11 shows the pressure drop across the reactor with turbulence promoter related to the value of the empty reactor as a function of the Reynolds number. Fig. 11 emphasizes the promissory performance of the EPM2 turbulence promoter due to its enhancement factor is between 4 and 6, similar to those of the SU-grid which is recognized as a particular good promoter [7], and the pressure drop is tolerable.

4. Conclusions

- The mass-transfer distribution is more significant when the reactor is empty. In this case, the local mass-transfer coefficient near the entrance is two and a half times higher than the mean value. By using a turbulence promoter the mass-transfer conditions become more uniform along the electrode length, depending on the promoter type.
- Special attention must be paid to the flow distributors at the entrance and exit regions of the reactor in order to avoid distortion of the mass-transfer results.
- The turbulence promoter must be placed along all the electrode length to obtain both a high mean mass-transfer coefficient as well as a more uniform distribution of the local coefficient.
- In double logarithmic coordinates, a nearly linear growth of the mean mass-transfer-coefficient takes place when the flow rate increases, for all turbulence promoters. The exponent of the Reynolds number was higher than 0.5 in all cases and the enlargement of the mass-transfer conditions strongly depends on the promoter type.
- Expanded plastics with an open structure, similar to EPM2, becomes attractive as turbulence promoters because of the enhancement and the major uniformity of the mass-transfer conditions compatible with an acceptable pressure drop across the reactor. These results open ways for improving cell design and exploitation conditions of electrochemical reactors for water disinfection.

Acknowledgements

The authors wish to thank German BMBF/AIF Köln (FKZ 1721X04), BMBF/DLR, MINCYT (Project AL/09/02), ANPCyT and CONICET of Argentina, Universidad Nacional del Litoral, Santa Fe, and Anhalt University, Köthen, for financial and technical support.

References

[1] D. Pletcher, F.C. Walsh, Industrial Electrochemistry, Chapman and Hall, London, 1993, p. 344 (Chapter 7).
[2] F. Cœuret, A. Storck, Elements de Genie Electrochimique, TEC&DOC, Paris, 1984, p. 148 (Chapter 3b).
[3] A. Storck, F. Cœuret, Mass and momentum transfer at a wall in the presence of turbulence promoters, Electrochimica Acta 22 (1977) 1155.
[4] A. Storck, D. Hutin, Mass transfer and pressure drop performance of turbulence promoters in electrochemical cells, Electrochimica Acta 26 (1981) 127.
[5] L. Carlsson, B. Sandegren, D. Simonsson, M. Rihovsky, Design and performance of a modular, multi-purpose electrochemical reactor, Journal of the Electrochemical Society 130 (1983) 342.
[6] O. Kuroda, S. Takahashi, M. Nomura, Characteristics of flow and mass transfer rate in an electrodialyzer compartment including spacer, Desalination 46 (1983) 225.
[7] M.M. Letord-Quemere, F. Cœuret, J. Legrand, Mass transfer at the wall of a thin channel containing an expanded turbulence promoting structure, Journal of the Electrochemical Society 135 (1988) 3063.
[8] T.R. Ralph, M.L. Hitchman, J.P. Milington, F.C. Walsh, Mass transport in an electrochemical laboratory filterpress reactor and its enhancement by turbulence promoters, Electrochimica Acta 41 (1996) 591.
[9] W.M. Taama, R.E. Plimley, K. Scott, Mass transfer rates in a DEM electrochemical cell, Electrochimica Acta 41 (1996) 543.
[10] C.F. Oduoza, A.A. Wragg, M.A. Patrick, The effects of a variety of wall obstructions on local mass transfer in a parallel plate electrochemical flow cell, Chemical Engineering Journal 68 (1997) 145.
[11] C.J. Brown, D. Pletcher, F.C. Walsh, J.K. Hammond, D. Robinson, Local mass transport effects in the FM01 laboratory electrolyser, Journal of Applied Electrochemistry 22 (1992) 613.
[12] C.J. Brown, D. Pletcher, F.C. Walsh, J.K. Hammond, D. Robinson, Studies of space-averaged mass transport in the FM01-LC laboratory electrolyser, Journal of Applied Electrochemistry 23 (1993) 38.
[13] M. Griffiths, C. Ponce de León, F.C. Walsh, Mass transport in the rectangular channel of a filter-press electrolyzer (the FM01-LC reactor), AIChE Journal 51 (2005) 682.
[14] C.P. Koutsou, S.G. Yiantsios, A.J. Karabelas, A numerical and experimental study of mass transfer in spacer-filled channels: Effects of spacer geometrical characteristics and Schmidt number, Journal of Membrane Science 326 (2009) 234.
[15] C. Rodrigues, V. Geraldes, M.N. de Pinho, V. Semião, Mass-transfer entrance effects in narrow rectangular channels with ribbed walls or mesh-type spacers, Chemical Engineering Science 78 (2012) 38.
[16] P. Shukla, K.K. Singh, P.K. Tewari, P.K. Gupta, Numerical simulation of flow electrolysers: Effect of obstacles, Electrochimica Acta 79 (2012) 57.
[17] M.E.H. Bergmann, Drinking water disinfection by in-line electrolysis: Product and inorganic by-product formation, in: C. Comninellis, G. Chen (Eds.), Electrochemistry for the Environment, Springer, New York, 2010, p. 163 (Chapter 7).
[18] A. Kraft, Electrochemical water disinfection: a short review, Platinum Metals Review 52 (2008) 177.
[19] E.R. Henquín, A.N. Colli, M.E.H. Bergmann, J.M. Bisang, Characterization of a bipolar parallel-plate electrochemical reactor for water disinfection using low conductivity drinking water, Chemical Engineering and Processing: Process Intensification 65 (2013) 45.
[20] D.J. Pickett, Electrochemical Reactor Design, 2nd ed., Elsevier, Amsterdam, 1979 (Chapter 4).
[21] A.N. Colli, J.M. Bisang, Validation of theory with experiments for local mass transfer at parallel plate electrodes under laminar flow conditions, Journal of the Electrochemical Society 160 (2013) E5.
[22] J.R. Selman, C.W. Tobias, Mass-transfer measurements by the limiting-current technique, Advance in Chemical Engineering 10 (1978) 211.
[23] T.K. Ross, A.A. Wragg, Electrochemical mass transfer studies in annuli, Electrochimica Acta 10 (1965) 1093.
[24] A.N. Colli, J.M. Bisang, Evaluation of the hydrodynamic behaviour of turbulence promoters in parallel plate electrochemical reactors by means of the dispersion model, Electrochimica Acta 56 (2011) 7312.
[25] F.M. White, Fluid Mechanics, 4th ed., McGraw Hill, Boston, 1998, p. 359 (Chapter 6).
[26] R.B. Bird, W.E. Stewart, E.N. Lightfoot, Transport Phenomena, 2nd ed., John Wiley & Sons, New York, 2002, p. 181 (Chapter 6).
[27] D. Pletcher, I. Whyte, F.C. Walsh, J.P. Millington, Reticulated vitreous carbon cathodes for metal ion removal from process streams. Part I: mass transport studies, Journal of Applied Electrochemistry 21 (1991) 659.
[28] Á. Frías-Ferrer, J. González-García, V. Sáez, C. Ponce de León, F.C. Walsh, The effects of manifold flow on mass transport in electrochemical filter-press reactors, AIChE Journal 54 (2008) 811.